Res Chem Intermed (2020) 46:987–997
DOI 10.1007/s11164-015-2298-5

A fluorescent probe for the detection of Hg^{2+} based on rhodamine derivative and modified CdTe quantum dots

Kun Zhang[1] · JiMei Zhang[1]

Received: 11 May 2015 / Accepted: 24 September 2015 / Published online: 4 November 2015

Abstract In this paper, Zn doped CdTe quantum dots (CdTe:Zn QDs) was synthesized and imbedded in silica particles via a reverse microemulsion method to form a QDs/silica core. It acted as a fluorescence energy donor to conjugate with fluorescence energy acceptor rhodamine B derivative and construct a fluorescence sensor based on the principle of fluorescence resonance energy transfer (FRET). Hg^{2+} ions induced the ring-opening reaction of the spirolactam rhodamine moieties, leading to the occurrence of FRET. The fluorescence probe was accomplished by detecting the fluorescence intensity at 521 nm and 577 nm, and it exhibited high selectivity, sensitivity and accuracy and the detection limit reached as low as 0.5 μM.

Keywords Fluorescence resonance energy transfer · Ratiometric derivative · Silica · CdTe:Zn QDs

Introduction

Heavy metal pollution, such as Hg^{2+}, Cd^{2+} and Pb^{2+}, is closely related to the human physiological processes and environment [1, 2]. Hg^{2+} existed in three forms: selemental mercury, mercury ions, and organic mercury [3]. Hg^{2+} or its derivatives were easily enter into human food chain and had very high affinity for thiol groups

Electronic supplementary material The online version of this article (doi:10.1007/s11164-015-2298-5) contains supplementary material, which is available to authorized users.

✉ JiMei Zhang
zhangjimei6d311@163.com

Kun Zhang
zyzk0510@163.com

[1] State Key Laboratory of Hollow Fiber Membrane Materials and Membrane Process, Tianjin Polytechnic University, Tianjin 300387, People's Republic of China

in the living body, thus producing the thiolate that leading to the functional disorders of cells [4, 5].

At present, the common ways to detect Hg^{2+} mainly include cold-vapor atomic absorption spectroscopy [6, 7], fluorescence spectroscopy [8–10], UV–vis spectrometry [11]. However, these methods were inconvenient, so developing inexpensive and simple methods to detect Hg^{2+} had obtained more attention [9]. Among these methods, fluorescence spectroscopy had become an effective way to detect metal ions due to its simplicity and high sensitivity [10–12]. Much attentions had been paid to fluorescent nanosensors in the fields of biological detection, environmental monitoring, cell imaging, drug delivery, disease diagnosis [13, 14].

Recently, FRET systems built in organic or inorganic particles were found to be water-soluble and could enhance the fluorescence intensity [15–17]. As a unique luminescent semiconductor nano-crystals material, Quantum dots (QDs) had attracted much attentions in different fields [18–20]. Compared to traditional dyes, QDs exhibit numerous advantages such as broad excitation spectrum, narrow emission spectrum [21, 22], which made them as good donors in FRET processes [23].

In this paper, we demonstrated a approach to construct a fluorescence probe. In these fluorescence sensing systems, CdTe:Zn QDs were embedded into the silica core as the energy donor and rhodamine B derivative was linked on the particle surface as the Hg^{2+} probe. The Hg^{2+} can induce an efficient ring-opening reaction of the rhodamine in this nanoparticle-based sensing system where the probe performs as the FRET acceptor.

Experimental

Reagents

Rhodamine B, (3-aminopropyl) triethoxysilane (APTES), Tetraethyl orthosilicate (TEOS), and mercaptopropionic acid (MPA) were purchased from Alfa Aesar. Chloride salts of metal ions (Na^+, K^+, Ca^{2+}, Mg^{2+}, Fe^{2+}, Co^{2+}, Ni^{2+}, Cu^{2+}, Zn^{2+}, Pb^{2+}, Cd^{2+}, Hg^{2+}, Al^{3+}) were obtained from Sigma-Aldrich. Ethanol, triethylamine, toluene and methanol were the products of Tianjin Chemical Co. Ltd.

Tellurium powder and $CdCl_2{\cdot}2.5H_2O$ were the products of Sinopharm Chemical Reagent Co. Ltd, China. $NaBH_4$ were purchased from Fuchen Chemical Reagent Institute, China. A Hg^{2+} standard stock solution was prepared by dissolving 16.7 mg of $Hg(NO_3)_2{\cdot}0.5H_2O$ in 50 mL double deionized water (DDW) containing three drops of HNO_3 (2.0 mol L^{-1}).

Apparatus

1H NMR spectra were recorded on a Bruker Avance Digital 400 MHz NMR Spectrometer. The MS were obtained on a LCQ Advantage MAX LC–MS. The size distribution was measured on Malvern Nano-ZS90 particle size analyzer and the morphology of nanoparticles was measured using H-7650 transmission electron microscope (TEM). UV–vis spectra was recorded on a Helios-γ spectrophotometer and fluorescence spectra was tested on a Hitachi F-380 fluorescence spectrophotometer.

Synthesis of spirolactam rhodamine ($RHB\text{-}NH_2$) (compound 1)

The spirolactam Rhodamine B derivative (compound 1) was synthesized as follows [24]. 3.13 mmol rhodamine B was dissolved in 30 mL anhydrous methanol, followed by adding 4.8 mmol tris (2-amino ethyl) amine. Then, the mixture was heated to 80 °C. After cooling down to the room temperature, the methanol solution was removed by rotary evaporation. The organic layer was washed several times, dried with anhydrous magnesium sulfate and purified by column chromatography on silica gel (CH_2Cl_2/MeOH/Et_3N = 40:2:1) to give a grayish white powder with a yield of 78.5 %. The synthesis process was shown in Scheme S1. The product was characterized by NMR and MS shown in Figure S1–S2. ^1H NMR ($CDCl_3$, 400 MHz) δ:7.90 − 7.87 (m, 1H), 7.47 − 7.39 (m, 2H), 7.12 − 7.08 (m, 1H), 6.42 − 6.35 (m, 4H), 6.29 − 6.26 (m, 2H), 3.37 − 3.30 (m, 8H), 3.18 − 3.14 (m, 2H), 2.58 − 2.53 (t, 4H), 2.37 − 2.35 (t, 4H), 2.25 − 2.21 (t, 2H), 2.14 − 2.08 (t, 4H), 1.19 − 1.15 (t, 12H). ESI m/z [M+H^+] = 571.6.

Synthesis of ethoxysilane-linked $RHB\text{-}NH_2$ (probe precursor)

According to the previous method [24], 0.38 mmoL $RHB\text{-}NH_2$ was dissolved in the redistilled toluene, followed by quickly adding 0.2 mL APTES and 0.4 mL triethylamine. The mixture was refluxed for 12 h at 80 °C. The probe precursor was obtained after rotary evaporation and further purification by column chromatography on silica gel (CH_2Cl_2/CH_3OH = 5:1), giving 320 mg brownish oily liquid which a yield of 80 %. The synthesis process was shown in Scheme S1. The product was characterized by NMR and MS shown in Figure S3–S4. ^1H NMR ($CDCl_3$, 400 MHz) δ:7.89 − 7.83 (m, 1H), 7.45 − 7.42 (m, 2H), 7.10 − 7.08 (m, 1H), 6.40 − 6.34 (m, 4H), 6.13 − 6.08 (m, 2H), 5.14 − 5.13 (s, 4H), 3.74 − 3.63 (m, 12H), 3.31 − 3.17 (m, 8H), 3.05 − 2.96 (m, 4H), 2.23 (s, 4H), 2.01 (s, 2H), 1.71 − 1.61 (m, 4H), 1.33 − 1.09 (m, 30H), 0.71 − 0.63 (t, 4H). ESI m/z [M+H^+] = 1065.8.

Synthesis of CdTe:Zn QDs

The CdTe:Zn QDs were synthesized as follows [25, 26]: fresh NaHTe solution was added to the N_2-saturated $CdCl_2$ and $ZnCl_2$ mixture using MPA as the stabilizer. The molecular proportion of n_{Cd}:n_{Te}:n_{MPA} was set as 1:0.2:2.4 and the concentration of Cd^{2+} was 5.0 mM, at the same time, the proportion of n_{Cd}:n_{Zn} was kept as 1:1 and 1:0 to synthesize the CdTe and CdTe:Zn QDs.

Construction Hg^{2+} probe based on CdTe:Zn QDs/SiO_2 and rhodamine B derivatives

The CdTe:Zn QDs/SiO_2 core/shell nanoparticles were synthesized by a reverse microemulsion method [27]. 15 mL cyclohexane, 3.54 mL Triton X-100 and 3.6 mL n-hexanol were added into a round bottom flask. Then, 800 μL CdTe:Zn QDs were added with stirring for 30 min. The CdTe:Zn QDs nanoparticles was embed in silica after

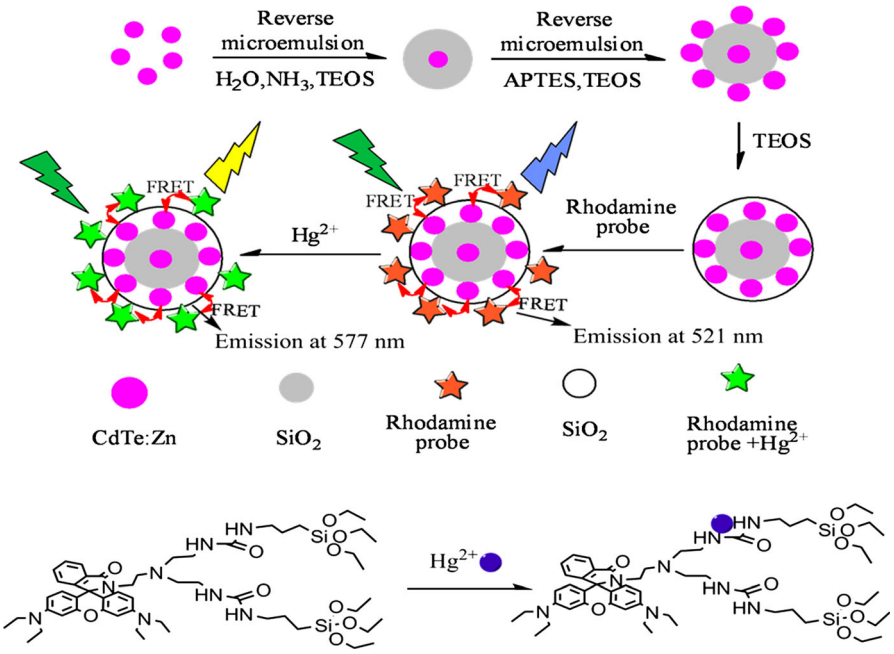

Scheme.1 Schematic illustration for the formation of silica particle-based ratiometric detection system for Hg^{2+} using FRET protocol

adding 200 μL TEOS and 120 μL, 25 % w.t. ammonia. After that, 40 μL APTES and 10 μL TEOS were added in the above system and stirred 12 h. The space layer could be formed outside each CdTe:Zn/silica QDs when 40 μL TEOS was added and stirred 12 h.

Finally, the rhodamine B derivative probe was immobilized on the silica surface of the microspheres after the probe was added and hydrolysis for 12 h. The surfactant materials was removed by centrifugation. The FRET system to detect Hg^{2+} was shown in Scheme 1.

Results and discussion

Fabrication of particle-based FRET system with CdTe:Zn QDs as the energy donor

In this study, a FRET-based rhodamine sensorwas constructed using CdTe:Zn QDs as the energy donor and rhodamine B derivative as probe. The fluorescence emission spectra of CdTe QDs and CdTe:Zn QDs was shown in Fig. 1. After Zn was incorporated in CdTe QDs, the fluorescence intensity enhanced. A probe precursor was constructed using an organic fluorophore to silica precursor by covalently conjugating (see Scheme S1 and Fig. S1). At the same time, the synthetic conditions were optimized to obtained CdTe:Zn QDs that made their emission

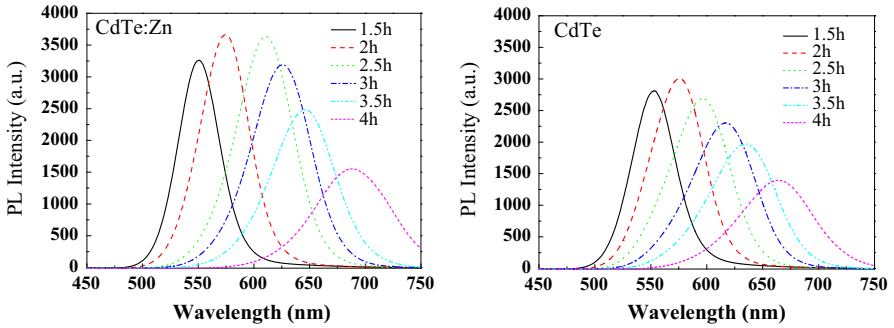

Fig. 1 The Fluorescence emission spectra of CdTe:Zn QDs and CdTe QDs

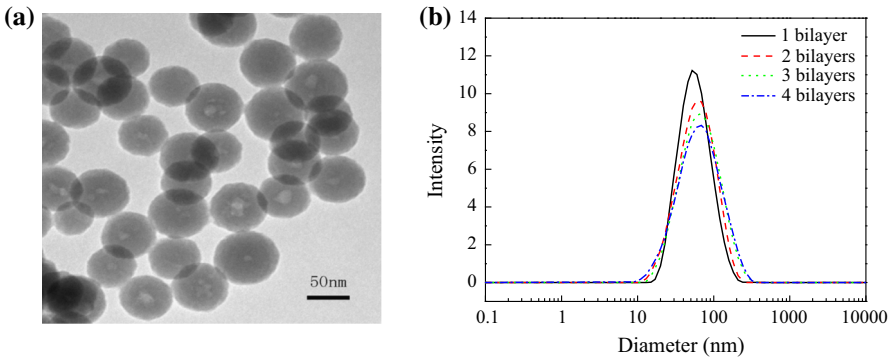

Fig. 2 TEM image of the fluorespheres(**a**) and particle size distribution (**b**)

spectrum overlap the absorption spectrum of receptor, so that the CdTe:Zn QDs can transfer their exited state energy to the acceptors, and FRET process occurred.

The CdTe:Zn QDs were embedded into silica particles and an amino group was modified to form a ultrathin layer. The Hg^{2+} probe was deposited on the CdTe:Zn QDs/silica nanoparticles surfaces to obtain QDs-containing silica nanoparticles. The morphology of the nano-composites were shown in Fig. 2a, where the particles were spherical and quite uniform in size distribution, and CdTe:Zn QDs were observed. The diameter distribution was shown in Fig. 2b. the averaged diameter of the particles were 58.18 nm, 59.23 nm, 61.4 nm and 61.8 nm. After coated a probe layer onto CdTe:Zn QDs/silica particles, it didn't cause detectable increase in the particle diameter.

Spectroscopic properties of CdTe:Zn/SiO_2 nanoparticles

The change of fluorescence intensity before and after CdTe:Zn QDs wrapped silica was shown in Fig. 3. The QDs exhibited a maximum emission at 541 nm, and

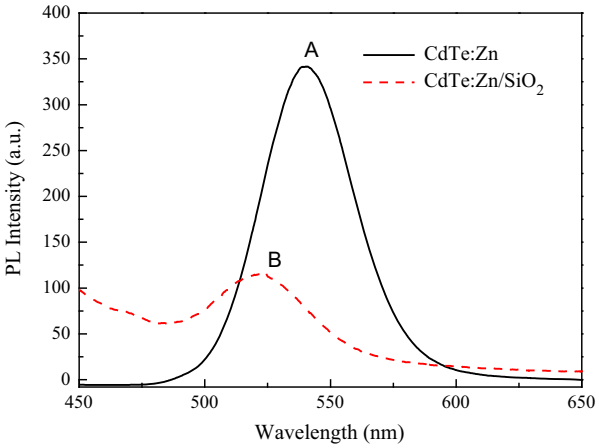

Fig. 3 The emission spectra for CdTe:Zn QDs and CdTe:Zn/SiO_2 nanocomposites

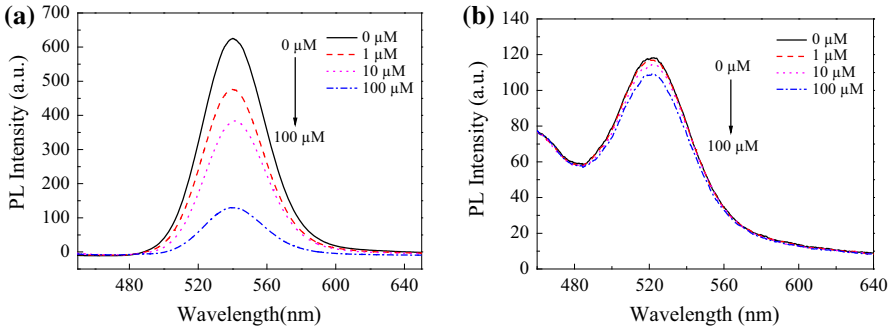

Fig. 4 The effect of Hg^{2+} on the fluorescent emission of CdTe:Zn QDs without (**a**) or with (**b**) a positively charged spacer layer on silica core

fluorescence intensity decreased after silica wrapped QDs, at same time, the maximum emission wavelength exhibited a moderate blue shift (20 nm) to 521 nm.

The Hg^{2+} radius was small and easy to penetrate into SiO_2 nanoparticles, leading to the fluorescence emission quenching effect of CdTe:Zn QDs. In order to detect Hg^{2+}, it is necessary to prevent Hg^{2+} from quenching the emission of the donor. We placed a positively charged ultrathin spacer layer between the QDs (containing particle core) and the probe layer to solve this problem. The spectroscopic properties of the QDs/silica with or without the spacer layer were shown in Fig. 4. It can be seen that, with the increasing of Hg^{2+}, the fluorescence intensity decreased. The QDs had great fluorescence quenching effect with the existence of a small amount of Hg^{2+}, especially the concentration of Hg^{2+} reached 100 μM. However, under the protection of the spacer by modifying amino group, the fluorescence intensity decreased and emission peak position almost had no change. In addition,

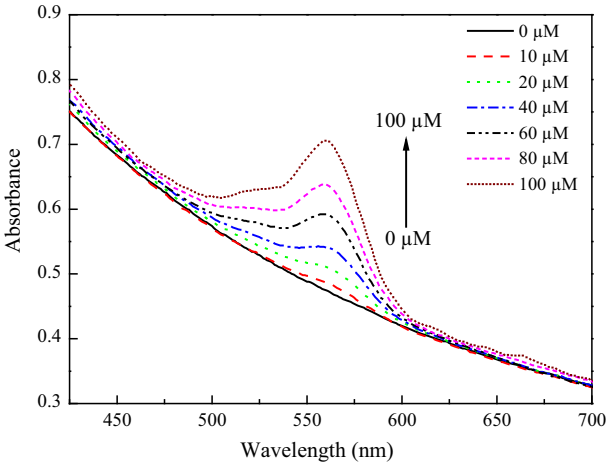

Fig. 5 The absorption spectra of fluorescence ratio probe with the addition of Hg^{2+}

the thickness of the spacer layer can be controlled by changing the reaction condition so that the FRET process may occur from the QDs in the particle core to the acceptor on the surface of the particle-based sensor. The absorption spectra of QDs/silica dispersion (with probe layer) with addition of Hg^{2+} at pH = 7.0 HEPES was shown Fig. 5. Before addition of Hg^{2+}, there was only a broad absorption profile, corresponding to the QDs/position of absorption in silica. With the Hg^{2+} concentration increased, a new absorption peak arisen at 560 nm, owing to the ring-opened of the rhodamine B derivative. This process indicated that the probe was incorporated on the nanoparticle surface and the existence of Hg^{2+} leading to the probe changing from the spirolactam state to ring-opened, which meant that rhodamine B derivative had a strong recognition effect on Hg^{2+}.

Fluorescent probe based on FRET for Hg^{2+} detection

The fluorescence probe was carried in HEPES (pH = 7.0). The change of the fluorescence intensity in Fig. 6a and the working curve was shown in Fig. 7. In the absence of Hg^{2+}, excite the nanoparticle dispersion at 410 nm only appeared a single fluorescence emission peak at 521 nm. When Hg^{2+} concentration was increased, the fluorescence intensity (I_{521}) gradually decreased and a acceptor emission peak occurred at 577 nm, corresponding to the fluorescence emission of rhodamine B derivative, which indicated that the rhodamine B derivative from the closed loop state turned to be open. Moreover, the color of the fluorescence changed from green (QDs) to orange (rhodamine B) after adding Hg^{2+}, as shown in Fig. 6b.

In the absence of Hg^{2+}, the fluorescence intensity ratio value (I_{577}/I_{521}) was 0.192, and increased to 3.54 after adding 100 μM Hg^{2+}. This ratio probe achieved linear detection in Hg^{2+} range from 0 μM to 10 μM and linear regression equation was $I_{577}/I_{521} = 0.9898C + 0.22752$, $R^2 = 0.9923$, which showed the fluorescence

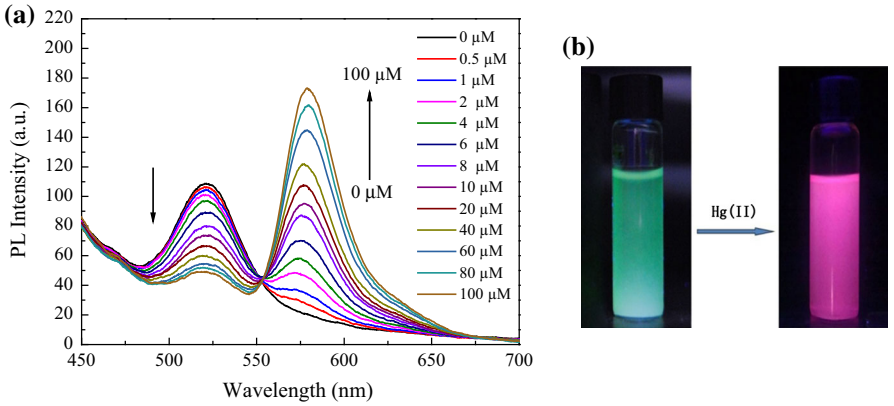

Fig. 6 The fluorescence spectra for fluorescent probes in pH = 7.0 HEPES buffered water upon addition different concentrations of Hg^{2+} (λ_{exc} = 410 nm) (**a**) Photographs of fluorescence for the CdTe:Zn QDs/silica nanocomposites dispersed in HEPES buffered solution (pH = 7.0) with or without Hg^{2+} under a 365 nm UV lamp (**b**)

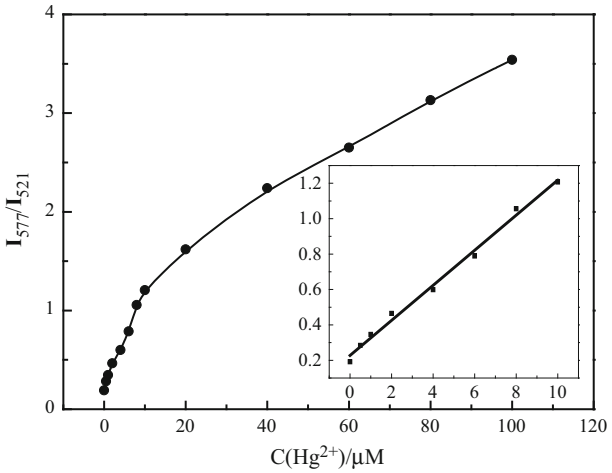

Fig. 7 Plot of fluorescence intensity ratio (I_{577}/I_{521}) versus Hg^{2+} concentration for the ratiometric sensor based on CdTe:Zn QDs/silica nanocomposites and inset shows the linear response at low Hg^{2+} concentration

probe could quantitatively and sensitively detect Hg^{2+} and detection limit was 0.5 μM.

According to the principle of FRET, the rate of energy transfer mainly depended on two factors, the spectral overlap and distance between the donor and acceptor moieties. The overlap of the emission spectra of QDs/silica and absorption spectra of ring-opened rhodamine B (Figure S5) indicated that the two fluorophores constituted a donor–acceptor pair of an energy transfer system.

According to the Förster non-radiative energy transfer theory [16], the FRET process can take place between a donor and an acceptor within a distance in the range of $R_0 \pm 50\ \%R_0$, where R_0 is the Förster critical distance. For this fluorescence system, the Förster critical distance R_0 was calculated as 1.1 nm (see the Supporting Information).

The selectivity and interference of the ratio probe

Selectivity is a very important parameter to evaluate the performance of the fluorescence sensing system. To evaluate this parameter, two experiments were carried out to detect the fluorescence intensity with Hg^{2+} and other metal ions co-existing, and the results were shown in Fig. 8a. After 100 μM Hg^{2+} was added, the fluorescence intensity increased compared to the blank sample (no ion was added), whereas some other metal ions lead to slight fluorescence intensity change. Overall, the ratio of the probe can efficiently achieve specific detection of Hg^{2+}.

The anti-interference ability of the ratio probe was also examined and results were shown in Fig. 8b. The co-existence of all selected metal ions didn't interfere with Hg^{2+}, which indicated that these coexistent ions had negligible interfering effect on Hg^{2+} sensing by the QDs/silica. Thus, Hg^{2+} selective binding and the FRET 'turn-on' can take place in the presence of all the competitive coexisting metal ions.

Effect of pH value on fluorescence biosensor

The pH had a significant effect on the fluorescence sensor. The effect on the fluorescence intensity ratio (I_{577}/I_{521}) in the absence or presence of 100 μM Hg^{2+} was shown in Fig. 9. With the absence of the Hg^{2+}, the rhodamine B derivatives remained in the spirolactam structure state and the fluorescence intensity ratio (I_{577}/I_{521}) hardly changed in the pH range from 1.0 to 13.0. On the contrary, the I_{577}/I_{521} increased between pH = 5.0 and pH = 8.0 in the presence of Hg^{2+}, indicating that the Hg^{2+} induced the ring-opening of the rhodamine B derivatives. In summary,

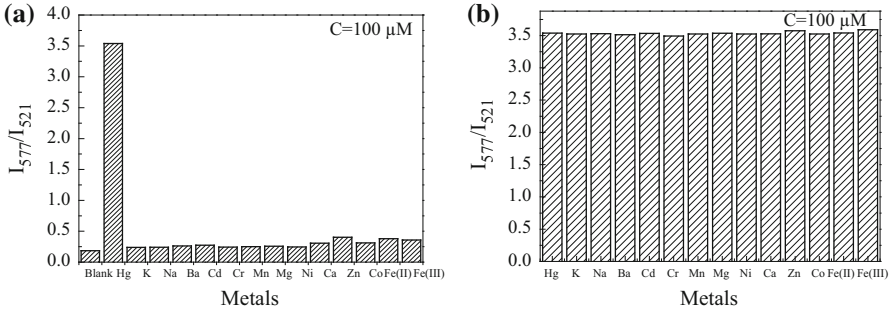

Fig. 8 Fluorescence intensity ratio (I_{577}/I_{521}) upon addition of 100 μM different metal ions respectively (**a**); fluorescence intensity ratio (I_{577}/I_{521}) in the presence of 100 μM of Hg^{2+} with 100 μM various other metal cations coexisting respectively (**b**) (λ_{exc}: 410 nm, pH = 7.0 HEPES)

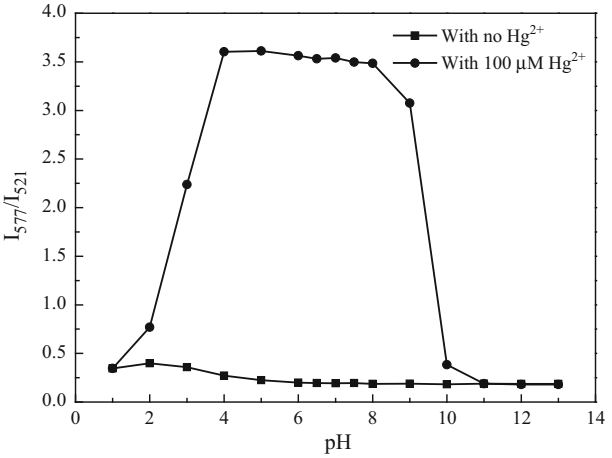

Fig. 9 The effect of pH on the fluorescence intensity of I_{577}/I_{521} in the absence or presence of 100 μM Hg^{2+}

when the ratio of the probe in weak acid to slightly alkaline condition (pH = 5.0–8.0), the probe remained fairly stable and could be used to detect Hg^{2+} accurately.

Conclusion

In summary, CdTe:Zn QDs were synthesized and embedded into silica nanoparticles to obtain multi-layers fluorescence nanospheres. Using these nanospheres as energy donor, a selective and sensitive fluorescent sensor has been designed to accurately detect Hg^{2+}. The results showed the probe was capable of detecting Hg^{2+} at a concentration as low as 0.5 μM and had good selectivity and anti-interference ability.

Acknowledgments This work was financially supported by the National Natural Science Foundation of China(NO. 21106101), National High Technology Research and Development Program of China (NO. 201406017), Tianjin Youth Science Foundation (NO. 13JCQNJC06300).

References

1. T.P. Flaten, Brain Res. Bull. **55**, 187 (2001)
2. D. McLachlan, T.P. Kruck, W.J. Lukiw, S.S. Krishnan, CMAJ. Can. Med. Assoc. J. **145**, 793 (1991)
3. Y. Chen, S. Mu, J. Lumin. **145**, 760 (2014)
4. Z. Dong-sheng, Z. Da-shun, S. Hai-yan, K. Zhang, Spectrochim. Acta Part A Mol. Biomol. Spectrosc. **118**, 1062 (2014)
5. Y. Jing-po, L. Fei, C. Jing, Y. Jin-di, Microporous Mesoporous Mater. **202**, 175 (2015)
6. J. Guzmán-Mar, L. Hinojosa-Reyes, A. Serra, A. Hernández-Ramírez, V. Cerdà, Anal. Chim. Acta **708**, 11 (2011)
7. Y. Zhang, S.B. Adeloju, Anal. Chim. Acta **721**, 22 (2012)

8. G. Xiang, L. Li, X. Jiang, L. He, L. Fan, Anal. Lett. **46**, 706 (2013)
9. H. Tao, X. Liao, M. Xu, S. Li, F. Zhong, Z. Yi, J. Lumin. **146**, 376 (2014)
10. Z. Hong-Jing, G. Wu-Er, H. Su-Ping, X.-J. JIANG, W. Ling-Zhong. Chin. J. Anal. Chem. **37**, 1029 (2009)
11. G.D. Huy, M. Zhang, P. Zuo, B.-C. Ye, Analyst **136**, 3289 (2011)
12. C. Ma, F. Zeng, G. Wu, S. Wu, Anal. Chim. Acta **734**, 69 (2012)
13. G. Chen, F. Song, X. Xiong, X. Peng, Ind. Eng. Chem. Res. **52**, 11228 (2013)
14. L. Yuan, W. Lin, K. Zheng, S. Zhu, Acc. Chem. Res. **46**, 1462 (2013)
15. B. Ma, F. Zeng, F. Zheng, S. Wu, Chem. A Eur. J **17**, 14844 (2011)
16. B. Liu, F. Zeng, G. Wu, S. Wu, Chem. Commun. **47**, 8913 (2011)
17. C. Li, Y. Zhang, J. Hu, J. Cheng, S. Liu, Angew. Chem. **122**, 5246 (2010)
18. I.L. Medintz, H.T. Uyeda, E.R. Goldman, H. Mattoussi, Nat. Mater. **4**, 435 (2005)
19. N.Y. Morgan, S. English, W. Chen, V. Chernomordik, A. Russo, P.D. Smith, A. Gandjbakhche, Acad. Radiol. **12**, 313 (2005)
20. Y.-S. Xia, C.-Q. Zhu, Talanta **75**, 215 (2008)
21. L. Juan, M. Fang, L. Wen-You, H. Xi-Wen, Z. Yu-Kui, Spectrochim. Acta Part A (Mol. Biomol. Spectrosc.) **70**, 811 (2008)
22. H. Mattoussi, J.M. Mauro, E.R. Goldman, G.P. Anderson, V.C. Sundar, F.V. Mikulec, M.G. Bawendi, J. Am. Chem. Soc. **122**, 12142 (2000)
23. M. Lunz, A.L. Bradley, V.A. Gerard, S.J. Byrne, Y.K. Gun'ko, V. Lesnyak, N. Gaponik, Phys. Rev. B **83**, 115423 (2011)
24. M.H. Lee, S.J. Lee, J.H. Jung, H. Lim, J.S. Kim, Tetrahedron **63**, 12087 (2007)
25. H. Zhang, L.P. Wang, H.M. Xiong, L.H. Hu, B. Yang, W. Li, Adv. Mater. **15**, 1712 (2003)
26. Z. Dan, F. Yang, W. Haoyuan, H. Zhike, J. Mater. Chem. **21**, 13365 (2011)
27. L. Jing, C. Yang, R. Qiao, M. Niu, M. Du, D. Wang, M. Gao, Chem. Mater. **22**, 420 (2009)